SEMARAK ILMU PUBLISHING

CFD Letters

Journal homepage:
https://semarakilmu.com.my/journals/index.php/CFD_Letters/index
ISSN: 2180-1363

Heat and Mass Transfer of CNTs Blood-based Casson Nanoliquids MHD Flow over a Rotating Stretchable Disk with Magnetic Field and Heat Source

Jada Prathap Kumar[1], Jawali Channabasappa Umavathi[1], Appasaheb S. Dhone[2,*]

[1] Department of Mathematics, Gulbarga University, Kalaburagi-585 106, Karnataka, India
[2] Department of Mathematics, Sangameshwar College (Autonomous), Solapur-413 001, Maharashtra, India

ARTICLE INFO

Article history:
Received 31 March 2023
Received in revised form 23 April 2023
Accepted 21 May 2023
Available online 1 September 2023

Keywords:
MHD; SWCNTs and MWCNTs nanoparticles; Casson parameter; Blood; Heat source (Exponential space and thermal dependent); Rotating disk

ABSTRACT

Carbon nanotubes (CNTs) are being used in nanomedicine as drug delivery systems, particularly for the medical therapy of cancer. The CNTs are initially infused into the blood, which then travels to the tumour via waves generated by the artery walls in the presence of an outside influence, like a magnetic field. This article analyses the study of heat and mass transmission in a blood-based Casson nanoliquid MHD flow using single-wall (SW) and multi-wall (MW) carbon nanotubes (CNTs) on a rotating disc with a heat source and magnetic field effects. The suspension of both kinds of carbon nanotubes is accomplished using Casson blood. The spinning and extending of the disc cause the flow to be formed. The controlling nonlinear PDEs are transformed into nonlinear ODEs, and ODEs are resolved using the Runge-Kutta fourth-order approach in MATLAB's bvp4c package. By means of graphical representation, the effects of different model restrictions are highlighted for the following parameters: momentum, energy transport, concentration, microorganism profiles, drag coefficient, heat and mass transport rates, and motile density number. This study demonstrates that the fluid momentum of a single-walled CNTs-blood Casson nanofluid is relatively less impacted and that the heat profile of this nanofluid is more dominant than that of a multi-walled CNTs-blood nanoliquid. The outcomes further show that with higher levels of the volume fraction of nanoparticles, the friction factor and rate of heat transport are improved.

1. Introduction

The Coriolis force is an imaginary or pseudo force that affects objects moving inside of a frame of reference that spins in relation to another frame of reference. Electronic equipment, computer memory gadgets, turning machines, medical instruments, rotating processes, etc. are only a few examples of the many manufacturing domains and engineering sectors where the Coriolis force is crucial to the analysis of nanofluid in porous space. The Coriolis force plays a significant role in the fundamental flow manifestation. The Coriolis effect depends on momentum, the motion of the earth

* *Corresponding author.*
E-mail address: dhoneas@gmail.com (Appasaheb S. Dhone)

https://doi.org/10.37934/cfdl.15.9.116135

and movement of the liquid or body that has been diverted by the Coriolis force. When travelling far or quickly, the impact of this force is more noticeable. The coriolis effect describes how weather affects fast-moving objects like rockets and airplanes. The Coriolis effect is primarily responsible for determining the directions of predominant winds. Most notably, climate variability is greatly stimulated by the Coriolis force. Coriolis force was used by Bachok *et al.,* [1] to study the movement of nanoliquids and the transfer of heat across a disc saturated with a porous medium. Rashidi *et al.,* [2] described an entropy generation analysis for magneto-steady flow due to the application of nanomaterials and Coriolis force through a disc. Turkyilmazoglu [3] examined the heat transfer properties of five different nanoparticles over a revolving disc. The Coriolis force substantially influences the fluid flow properties in several geophysical and manufacturing uses, which causes the creation of secondary flows [4]. Bai *et al.,* [5] investigated the water graphene oxide nanofluid flow in the riser condensing tubes of the solar collector heat transmission using computational methods and two-phase modelling. Mondel et *al.,* [6] conducted a study on the effectiveness of wind energy as a source of electricity in Bangladesh. Firdaus *et al.,* [7] conducted a fundamental investigation on the high-rise building's wind energy potential. Okonkwo *et al.,* [8] examined three approaches that may be created and used to produce green hydrogen for refueling stations utilising photovoltaic (PV) systems. Tlili and Alharbi [9] has studied numerical simulation of a solar wall using PMC.

Iijima's [10] 1991 research was the first to reveal CNTs, which are long, lean carbon cylinders. CNTs are allotropic forms of carbon that belong to the buck-minster-fullerene structural family, which also comprises spherically shaped buckyballs. These are massive macro-molecules that stand out due to their distinctive size, form, and exceptional physical characteristics. The information given by the CNT, manufacturing company NTI includes that the CNT particles are capable of displaying a 15-fold increase in thermal conductivity, a 1000-times higher current carrying capacity than copper, are five times more elastic, and are 200 times stronger than steel. CNT utilisation is also environmentally friendly since carbon chains are present in them. Therefore, it is crucial to comprehend how carbon nanotubes affect both Newtonian and non-Newtonian fluid flow. Single-wall CNTs (SWCNTs) and multi-wall CNTs (MWCNTs) are the two fundamental forms of CNTs. The incredible importance of carbon nanotubes (CNTs) in a variety of disciplines, including nanotechnology, calcareous water, conductive polymers, air purification techniques, surplus robust filaments, flat-panel displays, bio-sensors, and many other, has led to the conclusion that they will be the innovative substance of the twenty-first century. The model of heat conductivity for CNT-base mixtures was investigated by Xue [11]. Hayat *et al.,* [12] studied the characteristics of CNTs in a stretching flow issue of Darcy-Forchheimer, melting heat and chemical reactions. Mahanthesh *et al.,* [13] examined the Marangoni convection- and heat radiation-impacted MHD nano-liquid flow incorporating CNT nano-particles. Raja *et al.,* [14] used a clever computing approach to define the MHD flow of CNTs nanoliquid with slip. Mahesh *et al.,* [15] studied the impact of suction and injection across a Marangoni boundary layer flow on MHD Casson fluid and thermal radiation on a permeable surface using single-wall and multiwall CNT models. Maranna *et al.,* [16] determined the 2D movement of a viscoelastic ternary nanofluid made of Silver (Ag)-SWCNTs-Graphene across a permeable constricting surface under the influence of radiation, slip parameters, and heat source/sink implications. Maranna *et al.,*[17] examined the impacts of a CNT magnetic field flow due to a stretched plate when Navier's slip is present. Maranna *et al.,* [18] examined the impact of radiation and Marangoni convective boundary conditions on the flow of ternary hybrid nanofluids in a porous medium with mass transpiration effect.

Cancer has numerous types and is a commonplace and pervasive disease worldwide. Traditional medicine and nanotechnology with nanoparticles are the two methods used to treat cancer are taken from Chen *et al.,* [19] and Morrison *et al.,* [20]. Surgery, radiation, and chemotherapeutic are

examples of traditional treatments that use high doses of radiation and medications to reduce tumours and kill cancer cells, respectively [21]. In the nanotechnology treatment process, various nanoparticles, including magnetic particles, carbon nanotubes, and gold particles, are employed to cure cancer. When the temperature exceeds 42–45^0 C, the cancerous tissues are killed because these particles behave such as heat sources in the presence of the applied magnetic field. Rajakarunakaran *et al.,* [22] analysed machine learning regression techniques for determining concrete compression strength. Aljaloud *et al.,* [23] researched the thermal behaviour and phase transition of a copper oxide-containing water nanofluid that is contained inside a porous metal cylinder. Aljaloud *et al.,* [24] investigated the temperature effect of cross-nanofluid bioconvection phenomena caused by stretched cylinders. AlDosari *et al.,* [25] investigated the computational modelling of drug release employing nanoparticles in cancer cells on 2-D materials using the molecular dynamics approach. Banawas *et al.,* [26] used a molecular dynamics simulation to investigate how the starting temperature and starting pressure affected the thermal and mechanical behaviour of reinforced calcium phosphate cements.

Casson fluid is frequently employed in the simulation of blood flow and ordinary life suspension and has a number of advantages over other fluid models. The Casson fluid model has been used by the majority of investigators to assess the characteristics of flow of blood in arteries. Copley [27] and Scott-Blair [28] used the Casson fluid model to illustrate the fundamental shear character of blood in veins. In their investigations on the behaviour of flow of blood, Casson [29] examined the accuracy of the Casson fluid model and discovered that the yield stress for blood is not zero at lower shear velocities. The effect of blood circulation in tubes with a size varying from 130 to 1000 mm can be precisely measured using the Casson fluid simulation, discovered by Merrill *et al.,* [30]. Mustafa *et al.,* [31] and Mustefa *et al.,* [32] studied the parallel free flow in the presence of the Casson fluid on a semi-infinite plane plate and in the field of stagnation point approaching a extending sheet. Singh *et al.,* [33] have explored the laminar boundary layer flow of an electrically conducting Casson fluid caused by a horizontally perforated sheet that is linearly contracting or expanding with mass transpiration. Mahabaleshwar *et al.,* [34] examined the impact of radiation across the flow of sticky Casson nanofluids on a linear extending/shrinking surface with a mass transport factor. Omar *et al.,* [35] present the analytical solution to the behaviour of the unsteady Casson fluid with the incorporation of heat radiation and chemical processes. ZainulAbidin *et al.,* [36] investigated the effect of non-Newtonian blood rheology and stenosis height on the solute dispersion mechanism in the cardiovascular system.

Magnetohydrodynamics is the study of the magnetic properties of electrically conducting fluids like liquid metals, saltwater, electro-lytes, etc. Alfevin [37], a Swedish electrical engineer, pioneered the MHD fields. MHD is a collection of equation sets, including Maxwell's, Navier-Stokes, fluid dynamics, and electromagnetic. The MHD mobility of radioactive material on Casson nanoliquid was investigated by Walelign *et al.,* [38]. The properties of MHD on Casson fluid have been investigated by Mahantesh *et al.,* [39]. It is used in a wide variety of industrial and geophysical settings, including nuclear reactors, cold plasma generators, etc. The extensive geophysical and engineering uses of liquid motion caused by the rotating disc, including centrifugal machine, the crystal formation process, the pumping of metals at high melting temperatures, thermal power producing systems, and air cleaning equipment, have maintained investigators interest in the subject. Von Karman interprets the flow produced by the rotating disk [40]. The amalgamated effects of temperature and mass transport in flow brought on by the rotation of a course, porous disc is studied by Turkyilmazoglu and Senel [41]. Regarding the issues with stretching surfaces, rotational flow today finds enormous importance because of multiple uses including gas turbine rotors, disc cleaners, rotating machinery, food production, rotor-stator systems, diagnostic equipment, rotating

machinery, and numerous others. Khan *et al.,* [42] examines the Casson blood-gold nanofluid flow that results from an elongated turning disk. A stretched disk's effect on nanofluid flow was studied by Mustafa *et al.,* [43]. The analytical study of a continuous flow of visco-elastic liquid and MHD flow of second-grade fluids due to prolonged sheets in a permeable media utilising the Cattaneo-Christov pattern has been investigated by Maranna *et al.,*[44]. Mahabaleshwar *et al.,* [45] researched the non-Newtonian MHD flow and heat transmission of a Cu-Al_2O_3/water hybrid nanofluid caused by a permeable extending/ shrinking surface. Mahabaleshwar *et al.,* [46] examined the magnetohydrodynamic axisymmetric flow of Casson fluid across a non-linear permeable surface that is stretching/shrinking. Prasad *et al.,* [47] investigated the impact of entropy creation on the MHD peristaltic transfer of Casson nanofluid in a vertical, non-uniform channel with the effects of magnetic field and convective circumstances.

Heat transfer has many uses in the areas of engineering and metallurgy. In the realm of fluid mechanics, heat transfer through an extending sheet is a crucial issue. Sumalatha and Bandari [48] observed that the source of heat and radiation factor improved the fluid temperature when they investigated the impact of changes in the heat source on the casson fluid travelling across a deformed surface. Gul *et al.,* [49] examined the magnetic impact on thin-film blood based CNTs nanofluid flow. Akber *et al.,* [50] analyzed the magnetic impact on the flow of SW- and MW-CNTs across a flowing permeable channel. The "thermal-diffusion (Soret) effect" is the term used to refer the mass flux caused by a thermal gradient. The "diffusion-thermo (Dufour)" impact is the name given to the energy flux brought on by concentration changes. According to Kafoussias *et al.,* [51], the Soret effect, for example, to separate isotopes and in mixtures of gases with very small and moderate molecular weights has been used. Numerous real-world implications of the Soret and Dufour effects are found in the fields of geotechnical and chemical engineering fields. In the current work, these variables are taken into account in the temperature and mass equations, respectively, because of the significant technical uses of Soret and Dufour effects in the sciences and engineering. The influence of Soret, Dufour, chemical processes, and heat radiation on combined convection stagnation point movement on an isothermal vertical sheet in a porous medium was examined by Olanrewaju and Gbadeyan [52] through mathematical model analysis. In a porous media, stable natural convection and mass transport motion across a semi-infinite vertical porous plate were investigated by Alam *et al.,* [53] for the impacts of Dufour and Soret. Vishalakshi *et al.,* [54] explored the three-dimensional flow of a fluid with heat exchange while being affected by a magnetic field and when there is a porous medium. Dero *et al.,* [55] investigated how the suction phenomena and thermal slip impacts affected radiated hybrid nanoparticles with a stability framework.

The current investigation, which is inspired by the earlier work, looks into the thorough analysis of blood-based Casson nanoliquids made of CNTs flowing through a rotating extendable disc under the influence of a magnetic field and a heat source. The primary concern of this work is to excogitate the flow features of blood flow with the inclusion of CNTs nanoparticles. In this regard, the Casson fluid with Xue model was adopted to simulate the transportation of blood flow over a stretchable turning disk. Matlab is faster and allows you to test complex algorithms immediately without recompilation. In this study, the slip velocity, MHD flow, heat and mass transfer, and CNTs for a rotating disc flow are also inspected. Such effects on a Casson nanofluid have rarely been considered in the literature. Examining the MHD flow of a blood-based Casson nanoliquid, including SWCNTs and MWCNTs, as it passed over a stretched sheet is the goal of the current work. The behaviour of the fluid flow and heat profiles against various physical restrictions was examined. The novelty of this study is to investigate the impact of volume fraction, stretching parameter, thermal and exponential space-based heat source factors, magnetic factor, Dufour number, Soret number, Schmidt number, and Casson parameter on velocity, heat, concentration, Nusselt number, skin friction coefficient, and

Sherwood number. The impacts of all limitations on disparate profiles are shown in graphs. The outcomes of the current investigation are more significant.

2. Mathematical Formulation

2.1 Physical Configuration

Consider the flow of blood-based carbon nanoliquids over an extendable rotating disk. The rotating and expansion of the disc are what generate the flow. The disc is positioned at $z=0$, rotating at a fixed angular speed Ω, whereas z is the axis perpendicular to the lower disk in the cylindrical co-ordinate system, with r and s acting as the radial and tangential axes, respectively. SWCNTs and MWCNTs are utilized with blood as the working fluid. There is no slippage betwixt the blood and CNTs because they are in a no-slip situation.

Let T and C represent the temperature and concentration, respectively, and let (u,v,w) signifies the variables of velocities in the direction of (r,s,z), accordingly. At the surface of the disk, temperature and concentration are assumed to be T_f and C_w, respectively. Away from the disk contact, the free stream is maintained at fixed values of pressure p_∞, concentration C_∞, and temperature T_∞. The electrical field and hall current are not taken into account, and only the exogenous, unchanging magnetic flux is provided perpendicular to fluid motion with a fixed magnetic flux density of B_0. The boundary restrictions and physical issues are schematically shown in Figure 1.

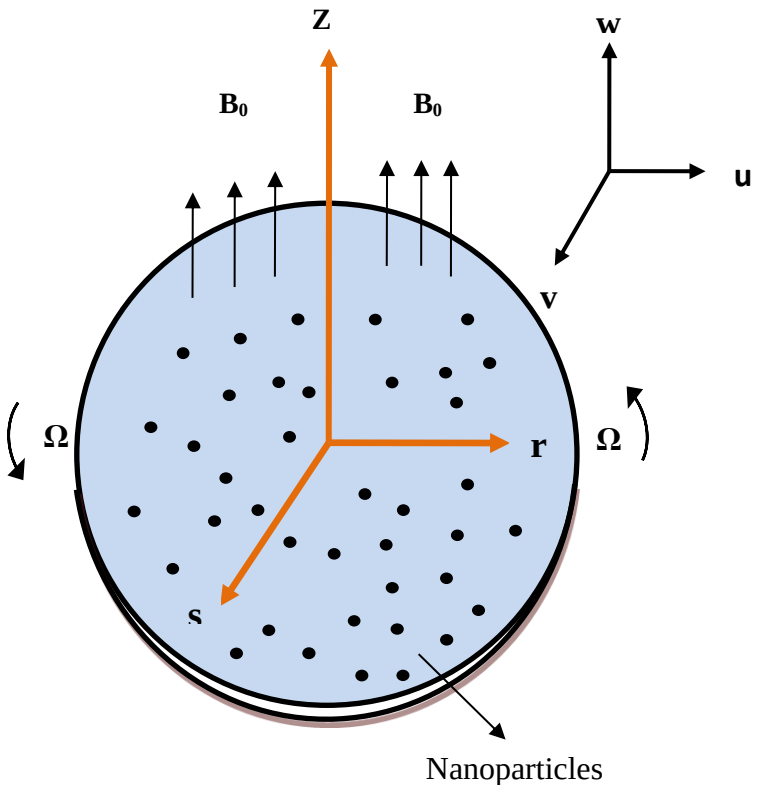

Fig. 1 Flow geometry

2.2 Regulating System and Boundary Constraints

The associated equations are obtained from [56-58].

Continuity equation,

$$\frac{\partial u}{\partial r}+\frac{u}{r}+\frac{\partial w}{\partial z}=0 \tag{1}$$

Momentum in radial direction

$$u\frac{\partial u}{\partial r}-\frac{v^2}{r}+w\frac{\partial u}{\partial z}+\frac{1}{\rho_{nf}}\frac{\partial p}{\partial r}=\frac{\mu_{nf}}{\rho_{nf}}\left(1+\frac{1}{\beta}\right)\left(\frac{\partial^2 u}{\partial r^2}+\frac{1}{r}\frac{\partial u}{\partial r}-\frac{u}{r^2}+\frac{\partial^2 u}{\partial z^2}\right)-\frac{\sigma B_0^2}{\rho_{nf}}u \tag{2}$$

Momentum in tangential direction

$$u\frac{\partial v}{\partial r}+\frac{uv}{r}+w\frac{\partial v}{\partial z}=\frac{\mu_{nf}}{\rho_{nf}}\left(1+\frac{1}{\beta}\right)\left(\frac{\partial^2 v}{\partial r^2}+\frac{1}{r}\frac{\partial v}{\partial r}-\frac{v}{r^2}+\frac{\partial^2 v}{\partial z^2}\right)-\frac{\sigma B_0^2}{\rho_{nf}}u \tag{3}$$

Vertical momentum

$$u\frac{\partial w}{\partial r}+w\frac{\partial w}{\partial z}+\frac{1}{\rho_{nf}}\frac{\partial p}{\partial z}=\frac{\mu_{nf}}{\rho_{nf}}\left(1+\frac{1}{\beta}\right)\left(\frac{\partial^2 w}{\partial r^2}+\frac{1}{r}\frac{\partial w}{\partial r}+\frac{\partial^2 w}{\partial z^2}\right) \tag{4}$$

Energy,

$$\begin{aligned}u\frac{\partial T}{\partial r}+w\frac{\partial T}{\partial z}&=\alpha_{nf}\left(\frac{\partial^2 T}{\partial r^2}+\frac{1}{r}\frac{\partial T}{\partial r}+\frac{\partial^2 T}{\partial z^2}\right)+\frac{Q_T^*}{\left(\rho C_p\right)_{nf}}\left(T-T_\infty\right)\\&+\frac{Q_E^*}{\left(\rho C_p\right)_{nf}}\left(T_f-T_\infty\right)\exp\left(-\left(\frac{\Omega}{\nu_f}\right)^{0.5}n z\right)+\frac{D K_T}{C_s C_{pf}}\left(\frac{\partial^2 C}{\partial r^2}+\frac{1}{r}\frac{\partial C}{\partial r}+\frac{\partial^2 C}{\partial z^2}\right)\end{aligned} \tag{5}$$

Concentration,

$$u\frac{\partial C}{\partial r}+w\frac{\partial C}{\partial z}=D\left(\frac{\partial^2 C}{\partial r^2}+\frac{1}{r}\frac{\partial C}{\partial r}+\frac{\partial^2 C}{\partial z^2}\right)+\frac{D K_T}{T_m}\left(\frac{\partial^2 T}{\partial r^2}+\frac{1}{r}\frac{\partial T}{\partial r}+\frac{\partial^2 T}{\partial z^2}\right) \tag{6}$$

With the limitations of the boundaries

$$\begin{aligned}&z=0:\ u=\frac{2-\chi}{\chi}\lambda\frac{\partial u}{\partial z}+s r,\ v=\frac{2-\chi}{\chi}\lambda\frac{\partial v}{\partial z}+\Omega r,\\&w=0,\ -k_{nf}\frac{\partial T}{\partial z}=h_f\left(T_f-T\right),\ C=C_w\\&z\to\infty:\ u\to 0,\ v\to 0,\ T\to T_\infty,\ C\to C_\infty\end{aligned} \tag{7}$$

Where, D is molecular diffusion coefficient, h_f for convective heat transmission coefficient, p is pressure, σ - electrical conductivity, χ - tangential momentum accommodation coefficient, ν - kinematic viscosity, β - Casson parameter, λ - velocity slip factor, n - exponential index, B_0 - constant magnetic flux density, C_p - heat capacity, C_s - concentration susceptibility, Q_T^* - thermal dependent heat source (THS) parameter, Q_E^* - exponential space dependent heat source (ESHS) coefficient, h_f - convective heat transfer coefficient, K_T - thermal-diffusion ratio, T_m -mean temperature of the fluid.

2.3 Nanofluid Effective Properties

The efficient nanofluid relationships provided by Xue [11] and discussed by Makinde and Animasaun [62,63] are of the following type:

$$\mu_{nf}=\frac{\mu_f}{(1-\varphi)^{2.5}},\quad \alpha_{nf}=\frac{k_{nf}}{(\rho C_p)_{nf}},\quad \rho_{nf}=(1-\varphi)\rho_f+\varphi\rho_s,$$
$$(\rho C_p)_{nf}=(1-\varphi)(\rho C_p)_f+\varphi(\rho C_p)_s,$$
$$\frac{k_{nf}}{k_f}=\frac{1-\varphi+2\varphi\frac{k_s}{k_s-k_f}\log\left(\frac{k_s+k_f}{2k_f}\right)}{1-\varphi+2\varphi\frac{k_f}{k_s-k_f}\log\left(\frac{k_s+k_f}{2k_f}\right)} \tag{8}$$

In Eq. (8), φ - nano-particle volume fraction, ρC_p is specific heat capacity, α - thermal diffusivity, μ is dynamic viscosity, ρ is density, k is thermal conductivity, Ω - constant angular velocity, the subscripts nf, f and s, respectively, symbolizes nonmaterial, base fluid and solid particles.

2.4 Similarity Transformations

To transform the governing PDEs into ODEs; we introduce the Von Karman's similarity transformations.

$$\xi=\left(\Omega/\nu_f\right)^{0.5}z,\quad u=\Omega r F(\xi),\quad v=\Omega r G(\xi),\quad w=\left(\Omega\nu_f\right)H(\xi),$$
$$p-p_\infty=2\mu_f\,\Omega\,p(\xi),\quad \theta(\xi)=\frac{T-T_\infty}{T_f-T_\infty},\quad \phi(\xi)=\frac{C-C_\infty}{C_w-C_\infty} \tag{9}$$

In these Eq. (9), ξ is non-dimensional variable, $F(\xi)$, $G(\xi)$, $H(\xi)$ denotes radial, tangential, and normal dimensionless velocity functions, respectively. $\theta(\xi)$ is non-dimensional temperature and $\phi(\xi)$ is non-dimensional concentration.

The PDE system consisting of Eq. (1) – Eq. (7) is condensed to the following ODEs by using Eq. (9):

$$\frac{dH}{d\xi}+2F=0 \tag{10}$$

$$\frac{1}{BD}\left(1+\frac{1}{\beta}\right)\frac{d^2F}{d\xi^2}-H\frac{dF}{d\xi}-F^2+G^2-\frac{M}{D}F=0 \tag{11}$$

$$\frac{1}{BD}\left(1+\frac{1}{\beta}\right)\frac{d^2G}{d\xi^2}-H\frac{dG}{d\xi}-2FG-\frac{M}{D}G=0 \tag{12}$$

$$\frac{E}{I\,\mathrm{Pr}}\frac{d^2\theta}{d\xi^2}-H\frac{d\theta}{d\xi}+\frac{Q_T}{I}\theta+\frac{Q_E}{I}\exp\left(-n\xi\right)+Du\frac{d^2\phi}{d\xi^2}=0 \tag{13}$$

$$\frac{1}{Sc}\frac{d^2\phi}{d\xi^2}-H\frac{d\phi}{d\xi}+Sr\frac{d^2\theta}{d\xi^2}=0 \tag{14}$$

With

$$\begin{aligned}&F\left(0\right)=c+A\left.\frac{dF}{d\xi}\right|_{\xi=0},\quad G\left(0\right)=1+A\left.\frac{dG}{d\xi}\right|_{\xi=0},\quad H\left(0\right)=0,\\&\frac{k_{nf}}{k_f}\left.\frac{d\theta}{d\xi}\right|_{\xi=0}=Bi\left(\theta\left(0\right)-1\right),\quad \phi\left(0\right)=1,\\&F\left(\infty\right)=G\left(\infty\right)=\theta\left(\infty\right)=\phi\left(\infty\right)=0\end{aligned} \tag{15}$$

The variables included in the equations mentioned above are:

$$\begin{aligned}&B=\left(1-\varphi\right)^{2.5},\quad D=1-\varphi+\varphi\frac{\rho_s}{\rho_f},\quad E=\frac{k_{nf}}{k_f},\\&I=1-\varphi+\varphi\frac{\left(\rho C_p\right)_s}{\left(\rho C_p\right)_f},\ M=\frac{\sigma B_0^2}{\rho_f\,\Omega},\quad \mathrm{Pr}=\frac{\left(\mu C_p\right)_f}{k_f},\\&Q_E=\frac{Q_E^*}{\left(\rho C_p\right)_f\Omega},\quad Q_T=\frac{Q_T^*}{\left(\rho C_p\right)_f\Omega},\quad Bi=\frac{h_f}{k_f}\left(\frac{\nu_f}{\Omega}\right)^{1/2},\\&Du=\frac{D\left(C_w-C_\infty\right)k_T}{C_sC_p\nu_f\left(T_f-T_\infty\right)},\quad Sc=\frac{\nu_f}{D},\quad Sr=\frac{D\left(T_f-T_\infty\right)k_T}{\nu_f\left(C_w-C_\infty\right)T_m},\\&c=\frac{s}{\Omega},\quad A=\frac{2-\chi}{\chi}\lambda\left(\frac{\Omega}{\nu_f}\right)^{1/2}\end{aligned} \tag{16}$$

In Eq. (16), the parameters M -magnetic parameter, Pr - Prandtl number, Q_T - THS/sink parameter, Q_E - ESHS/sink parameter, Bi - Biot number, Du - Dufour number, Sc - Schmidt number, Sr - Soret number, c - stretching parameter (measures the ratio of radial stretch to the swirl, and it ranges from 0 to 1, such that $c=0$ is the non-stretching case), and A signifies slip factor.

2.5 Physical Quantities

The drag force C_f , rate of heat transfer Nu , and mass transfer rate Sh are stated below:

$$C_f=\frac{\sqrt{\tau_{wr}^2+\tau_{wk}^2}}{\rho_f\left(\Omega r\right)^2},\quad Nu=\frac{r\,q_m}{k_f\left(T_f-T_\infty\right)},\quad Sh=\frac{r\,q_n}{C_w-C_\infty}, \tag{17}$$

The shear stresses along radial and tangential (τ_{wk} and τ_{wr}) axes at the disc's surface for Casson nanofluid are stated below:

$$\tau_{wr} = \left[\mu_{nf} \left(1+\frac{1}{\beta} \right) \left(\frac{\partial u}{\partial z} + \frac{\partial w}{\partial s} \right) \right]_{z=0}, \quad \tau_{wk} = \left[\mu_{nf} \left(1+\frac{1}{\beta} \right) \left(\frac{\partial v}{\partial z} + \frac{1}{r}\frac{\partial w}{\partial s} \right) \right]_{z=0},$$
$$q_m = -k_{nf} \left(\frac{\partial T}{\partial z} \right)_{z=0}, \quad q_n = -\left(\frac{\partial C}{\partial z} \right)_{z=0} \tag{18}$$

Here, q_m is heat flux, and q_n is mass flux at the disk surface.

Using Eq. (9) in Eq. (19) – Eq. (20), we have:

$$\mathrm{Re}^{1/2} C_f = \left(1+\frac{1}{\beta} \right) \frac{\sqrt{F'^2(0)+G'^2(0)}}{(1-\varphi)^{2.5}}, \quad \mathrm{Re}^{-1/2} Nu_x = -\frac{k_{nf}}{k_f}\theta'(0),$$
$$\mathrm{Re}^{-1/2} Sh = -\phi'(0) \tag{19}$$

Where $\mathrm{Re} = \dfrac{\Omega r^2}{\nu_f}$ is the local Reynolds number.

3. Results and Discussion

This section's graphical representations (Figure. 2 until Figure 14) examine the effects of relevant factors on the quantities $F(\xi)$, $G(\xi)$, $\theta(\xi)$, $\phi(\xi)$, drag force C_f, thermal exchange rate Nu_x, and mass transport coefficient Sh_x. Results have been obtained for both SW-CNTs (solid-lines) and MW-CNTs (dashed-lines). The relevant variables have the following default value until otherwise stated: $A=0.5$, $Bi=5.0$, $c=0.5$, $Du=0.1$, $M=0.5$, $n=0.5$, $\mathrm{Pr}=10$, $Q_E=Q_T=0.01$, $Sc=4.0$, $Sr=0.2$, $\beta=0.5$ and $\varphi=0.1$. The thermophysical characteristics of blood and CNTs are detailed in Table 1.

Table 1
List of the base fluid's and CNTs' physical characteristics [48,58]

Physical properties	SWCNT	MWCNT	Blood
ρ (kg m−3)	2600	1600	1050
Cp (J kg−1 k−1)	425	796	3617
k (Wm−1 k−1)	6600	3000	0.52

Figure 2(a) illustrates the impact of φ on the radial velocity $F(\xi)$ on the SW-CNT and MW-CNT added nanofluids. This graph clearly shows that as the φ parameter is magnified, the fluid momentum augments. Furthermore, as shown in Figure 2(a), the MWCNT-added nanofluids move at speeds that are higher than those of the SWCNT-added nanofluids. This information may be valuable for both manufacturing and medical uses. For instance, the research above suggests that MW-CNTs may reach the tumour more quickly than SW-CNT nanoparticles in the therapy of cancer.

Figure 2(b) depicts how the solid volume fraction φ responds to the tangential velocity distribution G. Greater φ results in an improvement in the velocity field G. In addition, the momentum profile G for MWCNTs is greater than that for SWCNTs. The overall reason is that the magnetic component with a negative sign is included in Eq. (12), and as a result, the azimuthal momentum is increasing. The drag force slows the flow in this scenario.

The relationship between the fluctuation in the heat profile $\theta(\xi)$ and the solid volume fraction φ is shown in Figure 2(c). The thermal energy profile $\theta(\xi)$ is raised for the solid volume fraction φ. This is because greater levels of the solid volume fraction cause the thermal layer thickness to grow. SWCNTs have a larger temperature distribution $\theta(\xi)$ than MWCNTs. This is a similar result reached by the authors in Akbar and Khan [59].

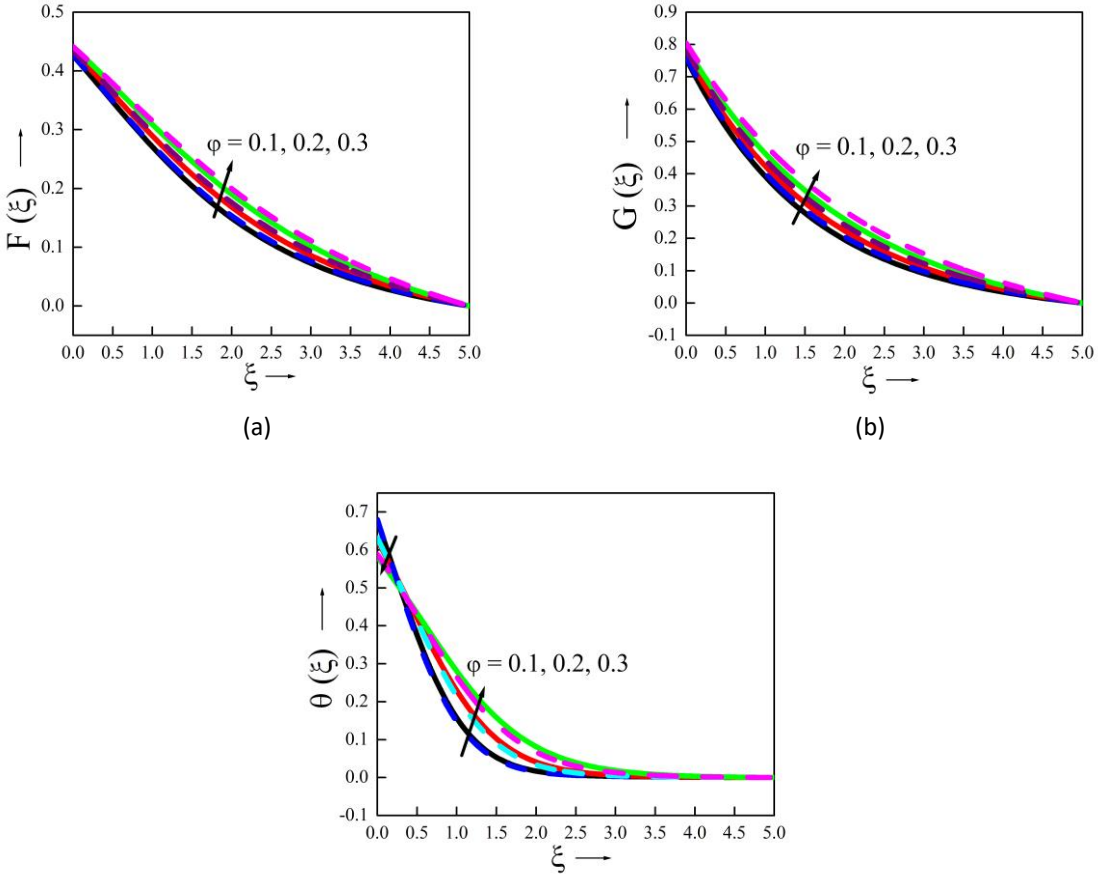

Fig. 2. Plots of φ versus (a) $F(\xi)$, (b) $G(\xi)$, (c) $\theta(\xi)$

It is evident from Figure 3 that the profile $\theta(\xi)$ surges during both Q_T and Q_E. Physically, bigger Q_T and Q_E result in more heat being produced in the fluid system, which causes $\theta(\xi)$ to rise. It is crucial to remember that the thermal field is stronger compared to the other situations when there is combined a thermal-based heat source (THS) and an exponential space-based heat source (ESHS). The exponential heat source factor, in particular, is significantly higher than the THS factor. As a result, the ESHS process is more appropriate for uses including heating processes, such as solar panels, atomic reactors, etc.

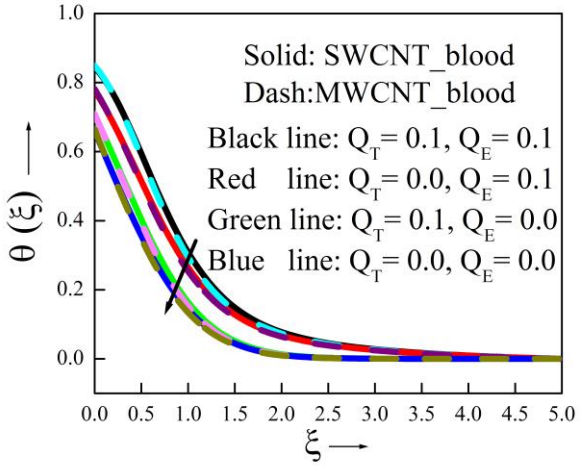

Fig. 3. Plots of $\theta(\xi)$ versus Q_T and Q_E

In Figure 4(a) to Figure 4(d), the effects of rising c values on $F(\xi)$, $G(\xi)$, $\theta(\xi)$ and $\phi(\xi)$ are depicted. The radial extending rate is measured by the factor c, which is specified as $c = s/\Omega$. Figure 4(a) exhibits that the radial momentum boundary layer thickens as the variable c increases. In fact, when c rises, the rate of radial expansion increases, accelerating flow in the radially outer direction. Mathematically, the disc extending force in the radial direction grows with c, which causes the radial velocity function $F(\xi)$ to grow for greater c. This is because the disc extending rate along the radial axis is exactly proportional to the extending strength factor c. Additionally, it is observed that the variation of $F(\xi)$ has a large impact on the revolving disk's surface. The results of tangential momentum have demonstrated progressive behaviour with growing c (see Figure 4(b)). Besides, it can be seen in Figure 4(c) that when the value of c rises, the heat profile reduces and the thermal boundary layer thins. Thus, in real-world applications, radial expansion of the disc aids in improving the revolving disk's cooling process. For water-based CNTs, a similar finding was reported in the published research by Mushtaq and Mustafa [61]. Figure 4(d) shows that for rising c, the concentration profile falls. Further, from these graphs it is noticed that both velocities ($F(\xi)$ and $G(\xi)$) are higher for MWCNT-nanoliquid than SWCNT-nanofluid.

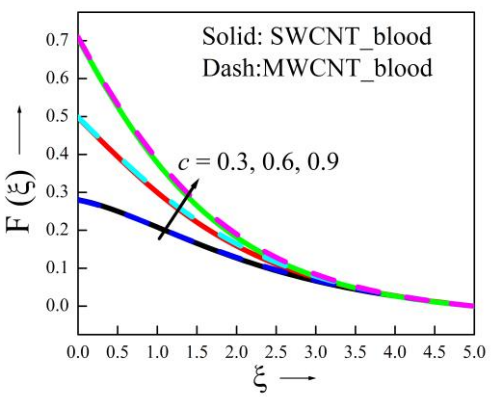

(a)

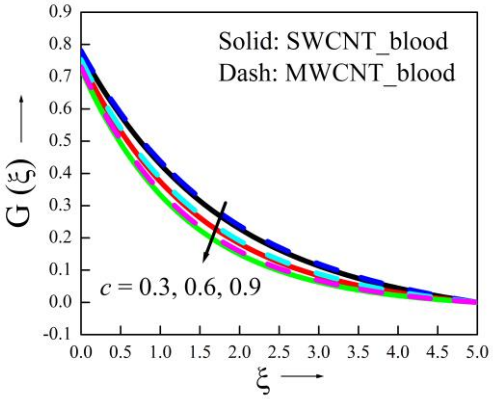

(b)

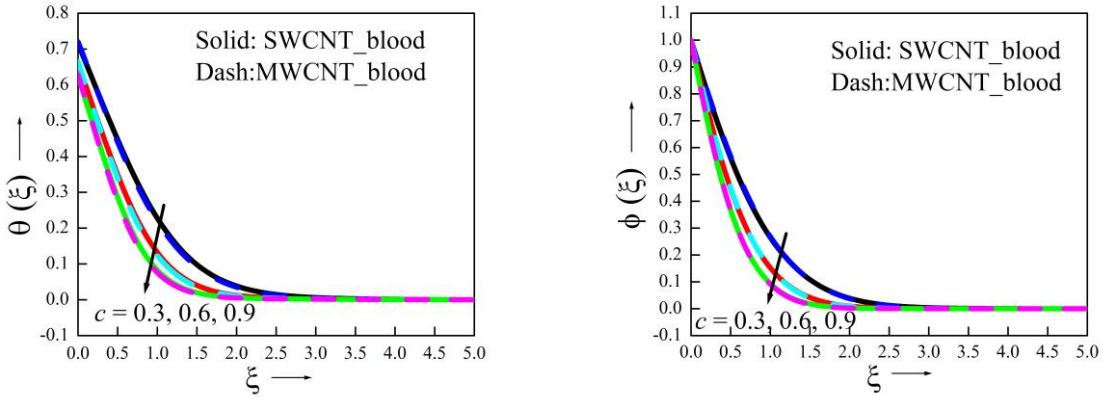

(c) (d)

Fig. 4. Plots of φ versus (a) $F(\xi)$ (b) $G(\xi)$ (c) $\theta(\xi)$ (d) $\varphi(\xi)$

The impact of the magnetic factor M on $F(\xi)$ and $G(\xi)$ velocities is presented in Figure 5(a) and Figure 5(b), respectively. The radial and tangential velocities for SW- and MW-CNT nanofluids fall as M rises. This is due to the strong resistive force (which resists liquid motion in nano-liquid flow) provided by the magnetic factor operating in the z direction, and this is what causes the $F(\xi)$ and $G(\xi)$ fluid momentums and the corresponding layer thickness to decrease. The flow velocities are likewise viewed to be significant in the zone of $0 \le \xi \le 2.0$ and to be diminishing along ξ. Furthermore, at the free stream, all curves converge to zero.

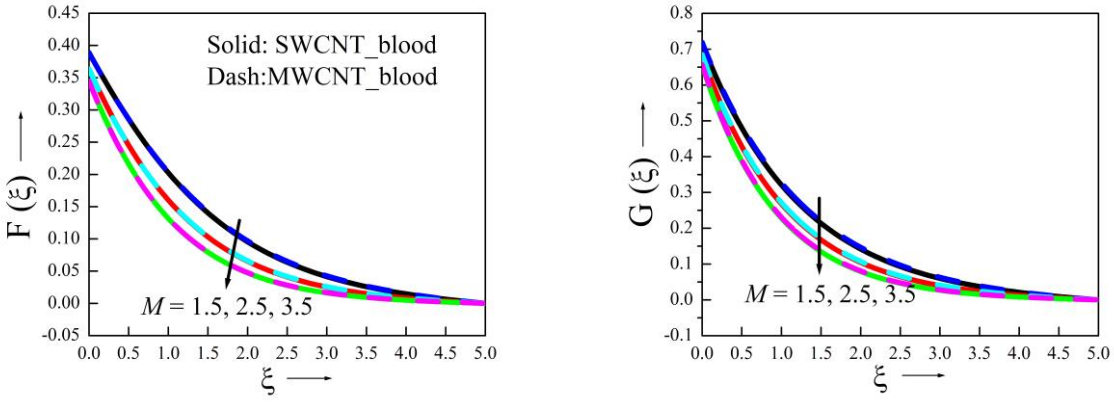

(a) (b)

Fig. 5. Plots of M versus (a) $F(\xi)$ (b) $G(\xi)$

The effects of M on $\theta(\xi)$ and $\phi(\xi)$ are interpreted in Figure 6(a) and Figure 6(b). The Lorentz theory states that the implemented magnetic field increases fluid heat and mass while diminishing the thickness of the boundary layer flow. This improvement occurs due to the reduction in velocities. Hence increasing value of M parameter increases the trend of temperature and concentration. In comparison to the MWCNT nanofluid, the SWCNT nanofluid exhibits lesser velocities and greater temperature dispersion. The reason behind this is SW-CNTs have more electrical conductivity in comparison with MW-CNTs. Aziz *et al.,* [60] and Mushtaq and Mustafa [61] both discovered a similar outcome.

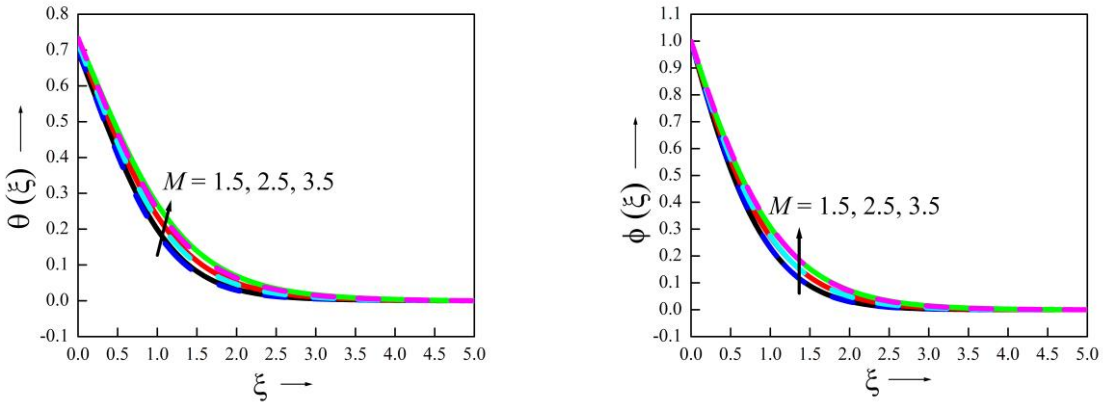

(a) (b)

Fig. 6. Plots of M versus (a) $\theta(\xi)$ (b) $\phi(\xi)$

Figure 7 depicts the influence of the Dufour number (Du) on temperature field ($\theta(\xi)$). For greater approximations of the Dufour number (Du = 0.0, 0.15, 0.3), the liquid temperature increases. An enhancement in energy flow is observed for higher values of the Dufour number because of the rise in concentration gradient that is accountable for increasing the temperature. One can see that the temperature near the lower disc is prominent, while in the upper half of the region it is zero.

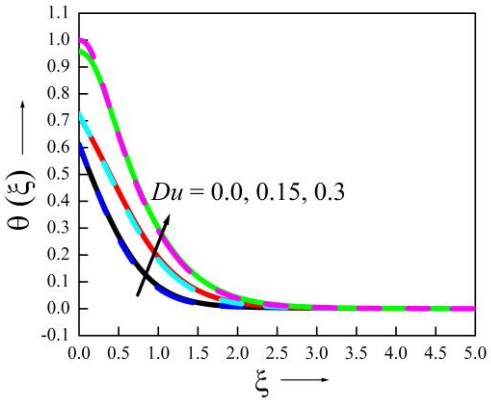

Fig. 7. Plots of Du versus $\theta(\xi)$

Figure 8 elucidates the impact of Soret number (Sr) on ($\phi(\xi)$). The concentration field is more pronounced in the lower half of the region for larger estimates of Soret number (Sr = 0.0, 2.0, or 4.0). It is because as Sr rises, the temperature gradient raises as well, leading to a larger convective flow. Consequently, the concentration profile ($\phi(\xi)$) gets higher. Moreover, in the upper half of the space between two discs, the concentration profiles are zero. Hence, it follows that the cross-diffusion impact can be used to regulate the rate of heat mass transport.

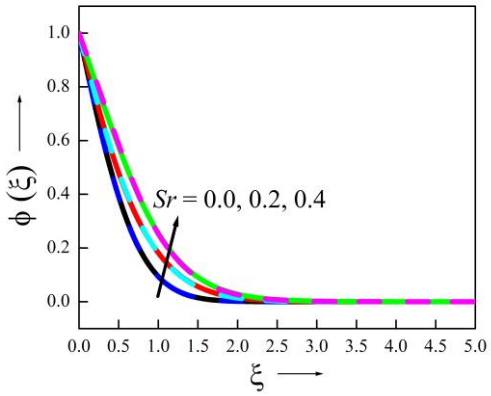

Fig. 8. Plots of Sr versus $\phi(\xi)$

The influence of Schmidt's number (Sc) on ($\phi(\xi)$) is pictured in Figure 9. The concentration profile narrows for greater values of Sc (Sc = 3.0, 5.0, or 7.0). The reason is that the bigger Sc lowers mass diffusivity, which lowers $\phi(\xi)$. In the upper half of the flow region concentration field converges to zero.

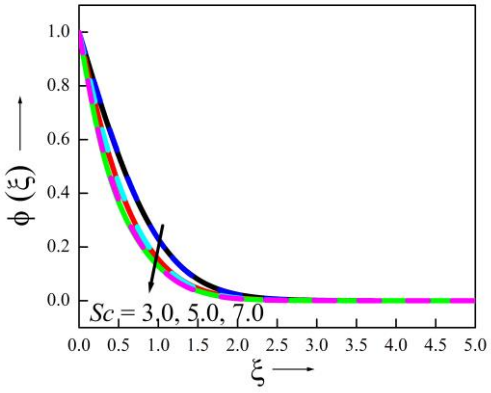

Fig. 9. Plots of Sc versus $\phi(\xi)$

The flow properties for various values of β are represented in Figure 10(a) and Figure 10(b). It is essential to mention that the β has a significant impact on the non-Newtonian behaviour of Casson fluid. As the value of β rises, the radial and tangential velocities drop as a result of the higher flow resistance. To put it another way, rising β is analogous to lowering the yield stress, which then lowers the fluid velocity. As β gets closer to infinity, the Casson problem is also transformed into a Newtonian problem. In addition, when CNT nanoparticles are suspended in a blood-based Casson nanoliquid, MWCNT move faster than SWCNT in the blood. The profiles converge to zero at the free stream.

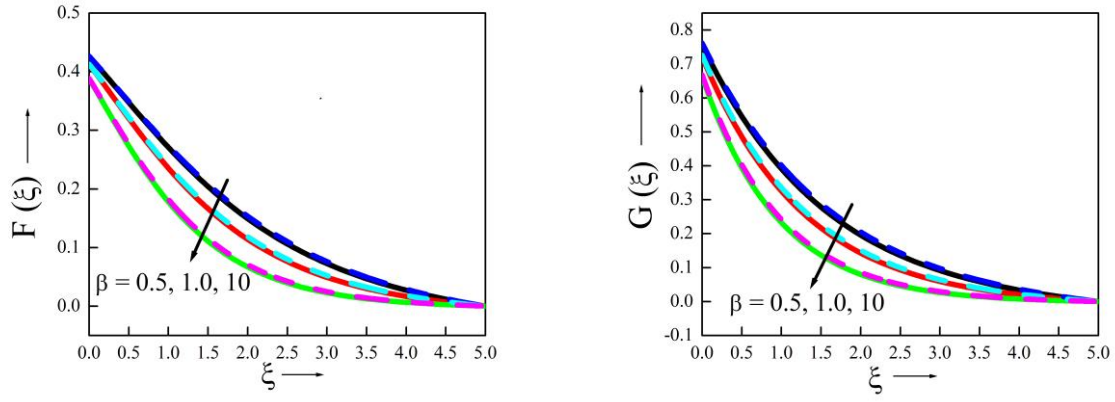

(a) (b)

Fig. 10. Plots of β versus (a) $F(\xi)$ (b) $G(\xi)$

The impact of β on the Casson nanofluid thermal performance is seen in Figure 11. It has been noted that when CNTs are added in blood-based Casson nanofluid, a spike in β values cause a rise in temperature. Moreover, it is obvious that the SWCNT nanoparticles have a greater heat than the MWCNT nanoparticles.

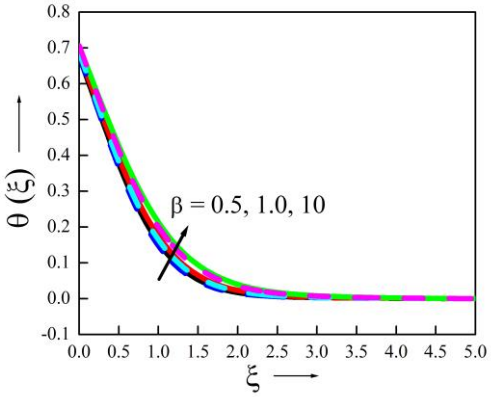

Fig. 11. Plots of β versus $\theta(\xi)$

From Figure 12, it is observed that the normalized drag force is increased with higher values of scaled stretching parameter c and decreased for larger values of Casson parameter β. It is evident from this graph that the SWCNT nanofluid has greater normalised drag force than the MWCNT nanofluid. Furthermore, the drag force at the free stream is high for minimal values of β. Both CNTs experience the same amount of drag for a significantly large value of the Casson parameter. The combined effect of M and φ on heat transfer rate is disclosed in Figure 13 for both SWCNT and MWCNT nanofluids. The rate of local heat exchange diminishes as M grows in value. In contrast hand, it gets better with greater values of φ. For a zero-volume fraction, both CNT curves are congruent. The Sherwood number, also known as the mass transfer rate, is an increasing function of Sc and reduces as Sr increases, as shown in Figure 14. The mass transfer rate is higher at the free stream, and the profiles are increasing linearly in the flow region.

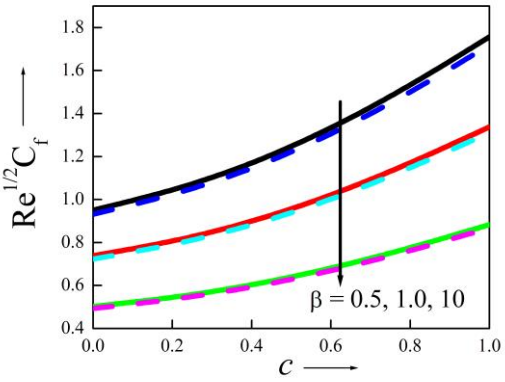

Fig. 12. Plots of β and c on $\mathrm{Re}^{1/2}\,C_f$

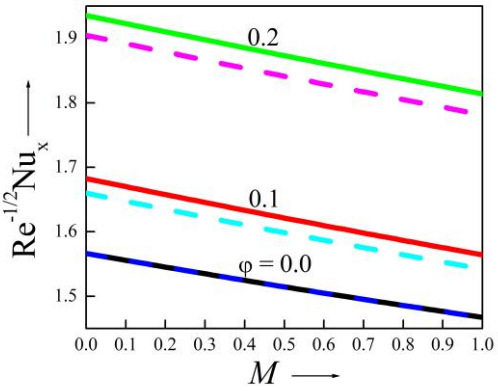

Fig. 13. Plots of φ and M on $\mathrm{Re}^{-1/2}\,Nu_x$

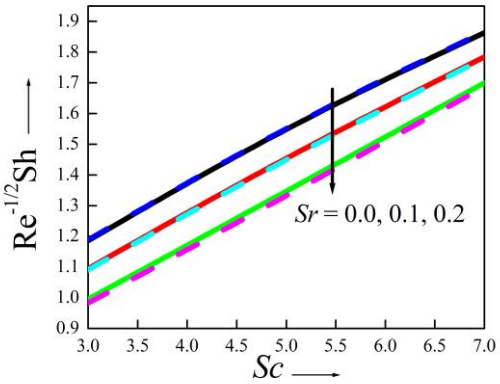

Fig. 14. Plots of Sc and Sr on $\mathrm{Re}^{-1/2}\,Sh$

4. Conclusion

The present study has investigated the fluid flow over a rotating extendable disc by dispersing CNTs in a blood based Casson nanoliquid in the presence of ESHS, THS, a magnetic field, and convective boundary conditions. The investigation is carried out by considering blood-based Casson nanofluid and SW- and MW- CNTs as the dispersing nanoparticles. The problem is solved numerically for the solutions of velocity, temperature, and concentration profiles by using the RK-4th order method with the bvp4c technique. Further analysis of the profiles affected by pertinent parameters is done by plotting the solutions graphically together with the comprehensive discussion. The following list includes the study's key findings:

i. The primary and secondary velocities are higher for MW-CNTs-nanoliquid compared to SW-CNTs-nanoliquid.
ii. The temperature field is improved in the presence of ESHS and THS aspects. Furthermore, the effect of ESHS is more prominent than the THS aspect.
iii. Stretching strength parameter enhances radial velocity while other profiles decline.
iv. Heat transfer rate is upraised for longer magnitude of φ for both cases of CNT-nanoparticles.
v. The mass transfer rate is increasing along Sc whereas decreases with Sr.

Acknowledgement
This research was not funded by any grant.

References
[1] Bachok, Norfifah, Anuar Ishak, and Ioan Pop. "Flow and heat transfer over a rotating porous disk in a nanofluid." *Physica B: Condensed Matter* 406, no. 9 (2011): 1767-1772. https://doi.org/10.1016/j.physb.2011.02.024
[2] Rashidi, M. M., S. Abelman, and N. Freidooni Mehr. "Entropy generation in steady MHD flow due to a rotating porous disk in a nanofluid." *International journal of Heat and Mass transfer* 62 (2013): 515-525. https://doi.org/10.1016/j.ijheatmasstransfer.2013.03.004
[3] Turkyilmazoglu, Mustafa. "Nanofluid flow and heat transfer due to a rotating disk." *Computers & Fluids* 94 (2014): 139-146. https://doi.org/10.1016/j.compfluid.2014.02.009
[4] Das, S., R. N. Jana, and O. D. Makinde. "Transient hydromagnetic reactive Couette flow and heat transfer in a rotating frame of reference." *Alexandria Engineering Journal* 55, no. 1 (2016): 635-644. https://doi.org/10.1016/j.aej.2015.12.009
[5] Bai, Jie, Dler Hussein Kadir, Moram A. Fagiry, and Iskander Tlili. "Numerical analysis and two-phase modeling of water Graphene Oxide nanofluid flow in the riser condensing tubes of the solar collector heat exchanger." *Sustainable Energy Technologies and Assessments* 53 (2022): 102408. https://doi.org/10.1016/j.seta.2022.102408
[6] Mondal, Mithun, Djamal Hissein Didane, Alhadj Hisseine Issaka Ali, and Bukhari Manshoor. "Wind Energy Assessment as a Source of Power Generation in Bangladesh." *Journal of Advanced Research in Applied Sciences and Engineering Technology* 26, no. 3 (2022): 16-22. https://doi.org/10.37934/araset.26.3.1622
[7] Firdaus, Nofirman, Bambang Teguh Prasetyo, Hasnida Ab-Samat, Heri Suyanto, and Rusjdi Halim. "Wind Energy Potential on A Highrise Building: A Preliminary Study." *Journal of Advanced Research in Fluid Mechanics and Thermal Sciences* 88, no. 3 (2021): 20-30. https://doi.org/10.37934/arfmts.88.3.2030
[8] Okonkwo, Paul C., Ikram Ben Belgacem, Manaf Zghaibeh, and Iskander Tlili. "Optimal sizing of photovoltaic systems based green hydrogen refueling stations case study Oman." *International Journal of Hydrogen Energy* 47, no. 75 (2022): 31964-31973. https://doi.org/10.1016/j.ijhydene.2022.07.140
[9] Tlili, Iskander, and Thamer Alharbi. "Investigation into the effect of changing the size of the air quality and stream to the trombe wall for two different arrangements of rectangular blocks of phase change material in this wall." *Journal of Building Engineering* 52 (2022): 104328. https://doi.org/10.1016/j.jobe.2022.104328
[10] Iijima, Sumio. "Helical microtubules of graphitic carbon." *nature* 354, no. 6348 (1991): 56-58. https://doi.org/10.1038/354056a0
[11] Xue, Q. Z. "Model for thermal conductivity of mixture of carbon-nanotube based composites." *Physisca B Condens Matter* 368 (2005): 302-307. https://doi.org/10.1016/j.physb.2005.07.024
[12] Hayat, Tasawar, Farwa Haider, Taseer Muhammad, and Ahmed Alsaedi. "On Darcy-Forchheimer flow of carbon nanotubes due to a rotating disk." *International Journal of Heat and Mass Transfer* 112 (2017): 248-254. https://doi.org/10.1016/j.ijheatmasstransfer.2017.04.123
[13] Mahanthesh, B., B. J. Gireesha, N. S. Shashikumar, and S. A. Shehzad. "Marangoni convective MHD flow of SWCNT and MWCNT nanoliquids due to a disk with solar radiation and irregular heat source." *Physica E: Low-dimensional Systems and Nanostructures* 94 (2017): 25-30. https://doi.org/10.1016/j.physe.2017.07.011
[14] Raja, Muhammad Asif Zahoor, Tuqeer Ahmed, and Syed Muslim Shah. "Intelligent computing strategy to analyze the dynamics of convective heat transfer in MHD slip flow over stretching surface involving carbon nanotubes." *Journal of the Taiwan Institute of Chemical Engineers* 80 (2017): 935-953. https://doi.org/10.1016/j.jtice.2017.08.016
[15] Mahesh, R., U. S. Mahabaleshwar, Emad H. Aly, and Oronzio Manca. "An impact of CNTs on an MHD Casson Marangoni boundary layer flow over a porous medium with suction/injection and thermal radiation." *International Communications in Heat and Mass Transfer* 141 (2023): 106561. https://doi.org/10.1016/j.icheatmasstransfer.2022.106561
[16] Maranna, T., U. S. Mahabaleshwar, L. M. Perez, and O. Manca. "Flow of viscoelastic ternary nanofluid over a shrinking porous medium with heat Source/Sink and radiation." *Thermal Science and Engineering Progress* 40 (2023): 101791. https://doi.org/10.1016/j.tsep.2023.101791
[17] Maranna, T., K. N. Sneha, U. S. Mahabaleshwar, Ioannis E. Sarris, and Theodoros E. Karakasidis. "An effect of radiation and MHD Newtonian fluid over a stretching/shrinking sheet with CNTs and mass transpiration." *Applied Sciences* 12, no. 11 (2022): 5466. https://doi.org/10.3390/app12115466

[18] Maranna, Thippaiah, Ulavathi S. Mahabaleshwar, and Michael I. Kopp. "The Impact of Marangoni Convection and Radiation on Flow of Ternary Nanofluid in a Porous Medium with Mass Transpiration." *Journal of Applied and Computational Mechanics* 9, no. 2 (2023): 487-497.
[19] Chen, Zou, Li Xia, Wei, Haigang, Wu, Siyuan, Song, Jing, Tang, Zhe, Luo Hailing, L. V. Xiaozhi, and Yilong Ai. "miR-375-NAT10 Axis Dysfunction Promotes Oral Cancer Development and Mediates Cdk7 Stabilizing and Cell Cycle Progression." (2021). https://doi.org/10.21203/rs.3.rs-718593/v1
[20] Morrison, Jo, Krishnayan Haldar, Sean Kehoe, and Theresa A. Lawrie. "Chemotherapy versus surgery for initial treatment in advanced ovarian epithelial cancer." *Cochrane Database of Systematic Reviews* 8 (2012). https://doi.org/10.1002/14651858.CD005343.pub3
[21] Abu-Dief, Ahmed M., Mohammed SM Abdelbaky, David Martínez-Blanco, Zakariae Amghouz, and Santigo García-Granda. "Effect of chromium substitution on the structural and magnetic properties of nanocrystalline zinc ferrite." *Materials Chemistry and Physics* 174 (2016): 164-171. https://doi.org/10.1016/j.matchemphys.2016.02.065
[22] Rajakarunakaran, Surya Abisek, Arun Raja Lourdu, Suresh Muthusamy, Hitesh Panchal, Ali Jawad Alrubaie, Mustafa Musa Jaber, Mohammed Hasan Ali et al. "Prediction of strength and analysis in self-compacting concrete using machine learning based regression techniques." *Advances in Engineering Software* 173 (2022): 103267. https://doi.org/10.1016/j.advengsoft.2022.103267
[23] Aljaloud, Amjad Salamah M., Kamel Smida, Hawzhen Fateh M. Ameen, M. A. Albedah, and Iskander Tlili. "Investigation of phase change and heat transfer in water/copper oxide nanofluid enclosed in a cylindrical tank with porous medium: A molecular dynamics approach." *Engineering Analysis with Boundary Elements* 146 (2023): 284-291. https://doi.org/10.1016/j.enganabound.2022.10.034
[24] Aljaloud, Amjad Salamah M., Leila Manai, and Iskander Tlili. "Bioconvection flow of Cross nanofluid due to cylinder with activation energy and second order slip features." *Case Studies in Thermal Engineering* 42 (2023): 102767. https://doi.org/10.1016/j.csite.2023.102767
[25] AlDosari, Sahar Mohammed, Saeed Banawas, Hevi Seerwan Ghafour, Iskander Tlili, and Quynh Hoang Le. "Drug release using nanoparticles in the cancer cells on 2-D materials in order to target drug delivery: A numerical simulation via molecular dynamics method." *Engineering Analysis with Boundary Elements* 148 (2023): 34-40. https://doi.org/10.1016/j.enganabound.2022.12.020
[26] Banawas, Saeed, Talib K. Ibrahim, Iskander Tlili, and Quynh Hoang Le. "Reinforced Calcium phosphate cements with zinc by changes in initial properties: A molecular dynamics simulation." *Engineering Analysis with Boundary Elements* 147 (2023): 11-21. https://doi.org/10.1016/j.enganabound.2022.11.033
[27] Copley, A. L. "Hemorheological aspects of the endothelium-plasma interface." *Microvascular Research* 8, no. 2 (1974): 192-212. https://doi.org/10.1016/0026-2862(74)90094-6
[28] Scott-Blair, G. W. "An equation for the flow of blood, plasma and serum through glass capillaries." *Nature* 183, no. 4661 (1959): 613-614. https://doi.org/10.1038/183613a0
[29] Casson, N. "Flow equation for pigment-oil suspensions of the printing ink-type." *Rheology of disperse systems* (1959): 84-104.
[30] Merrill, E. W., A. M. Benis, E. R. Gilliland, T. K. Sherwood, and E. W. Salzman. "Pressure-flow relations of human blood in hollow fibers at low flow rates." *Journal of Applied Physiology* 20, no. 5 (1965): 954-967. https://doi.org/10.1152/jappl.1965.20.5.954
[31] Mustafa, Meraj, Tasawar Hayat, Pop Ioan, and Awatif Hendi. "Stagnation-point flow and heat transfer of a Casson fluid towards a stretching sheet." *Zeitschrift für Naturforschung A* 67, no. 1-2 (2012): 70-76. https://doi.org/10.5560/zna.2011-0057
[32] Mustefa, M., T. Hayet, I. Pop, and A. Aziz. "Unstedy boundery layar flow of a Casson fluid impulsively startad moving flet plte." *Heat Transfer–Asian Ras* 40, no. 6 (2011): 563-76. https://doi.org/10.1002/htj.20358
[33] Singh, Jitender, A. B. Vishalakshi, U. S. Mahabaleshwar, and Gabriella Bognar. "MHD Casson fluid flow with Navier's and second order slip due to a perforated stretching or shrinking sheet." *Plos one* 17, no. 11 (2022): e0276870. https://doi.org/10.1371/journal.pone.0276870
[34] Mahabaleshwar, Ulavathi Shettar, Thippaiah Maranna, and Filippos Sofos. "Analytical investigation of an incompressible viscous laminar Casson fluid flow past a stretching/shrinking sheet." *Scientific Reports* 12, no. 1 (2022): 18404. https://doi.org/10.1038/s41598-022-23295-6
[35] Omar, Nur Fatihah Mod, Husna Izzati Osman, Ahmad Qushairi Mohamad, Rahimah Jusoh, and Zulkhibri Ismail. "Analytical Solution on Performance of Unsteady Casson Fluid with Thermal Radiation and Chemical Reaction." *Journal of Advanced Research in Numerical Heat Transfer* 11, no. 1 (2022): 36-41.
[36] ZainulAbidin, Siti Nurulaifa Mohd, Zuhaila Ismail, and Nurul Aini Jaafar. "Mathematical Modeling of Unsteady Solute Dispersion in Bingham Fluid Model of Blood Flow Through an Overlapping Stenosed Artery." *Journal of Advanced*

Research in Fluid Mechanics and Thermal Sciences 87, no. 3 (2021): 134-147. https://doi.org/10.37934/arfmts.87.3.134147
[37] Alfevin, D. Tabor. "Nature Publishing Group." *Nature Publishing Group.* (1942).
[38] Walelign, Tadesse, Eshetu Haile, Tesfaye Kebede, and Assaye Walelgn. "Analytical study of heat and mass transfer in MHD flow of chemically reactive and thermally radiative Casson nanofluid over an inclined stretching cylinder." *Journal of Physics Communications* 4, no. 12 (2020): 125003. https://doi.org/10.1088/2399-6528/abcdba
[39] Mahanthesh, B., and B. J. Gireesha. "Scrutinization of thermal radiation, viscous dissipation and Joule heating effects on Marangoni convective two-phase flow of Casson fluid with fluid-particle suspension." *Results in physics* 8 (2018): 869-878. https://doi.org/10.1016/j.rinp.2018.01.023
[40] Kármán, Th V. "Über laminare und turbulente Reibung." *ZAMM-Journal of Applied Mathematics and Mechanics/Zeitschrift für Angewandte Mathematik und Mechanik* 1, no. 4 (1921): 233-252. https://doi.org/10.1002/zamm.19210010401
[41] Turkyilmazoglu, M., and P. Senel. "Heat and mass transfer of the flow due to a rotating rough and porous disk." *International Journal of Thermal Sciences* 63 (2013): 146-158. https://doi.org/10.1016/j.ijthermalsci.2012.07.013
[42] Khan, Umair, Sardar Bilal, A. Zaib, O. D. Makinde, and Abderrahim Wakif. "Numerical simulation of a nonlinear coupled differential system describing a convective flow of Casson gold–blood nanofluid through a stretched rotating rigid disk in the presence of Lorentz forces and nonlinear thermal radiation." *Numerical Methods for Partial Differential Equations* 38, no. 3 (2022): 308-328.
[43] Mustafa, M., Junaid Ahmad Khan, T. Hayat, and A. Alsaedi. "On Bödewadt flow and heat transfer of nanofluids over a stretching stationary disk." *Journal of Molecular Liquids* 211 (2015): 119-125. https://doi.org/10.1016/j.molliq.2015.06.065
[44] Maranna, T., K. N. Sneha, U. S. Mahabaleshwar, and Basma Souayeh. "An impact of heat and mass transpiration on magnetohydrodynamic viscoelastic fluid past a permeable stretching/shrinking sheet." *Heat Transfer* 52, no. 3 (2023): 2231-2248. https://doi.org/10.1002/htj.22782
[45] Mahabaleshwar, U. S., Emad H. Aly, and T. Anusha. "MHD slip flow of a Casson hybrid nanofluid over a stretching/shrinking sheet with thermal radiation." *Chinese Journal of Physics* 80 (2022): 74-106. https://doi.org/10.1016/j.cjph.2022.06.008
[46] Mahabaleshwar, U. S., T. Maranna, L. M. Perez, and SN Ravichandra Nayakar. "An effect of magnetohydrodynamic and radiation on axisymmetric flow of non-Newtonian fluid past a porous shrinking/stretching surface." *Journal of Magnetism and Magnetic Materials* 571 (2023): 170538. https://doi.org/10.1016/j.jmmm.2023.170538
[47] Prasad, Kerehalli Vinayaka, Hanumesh Vaidya, Fateh Mebarek Oudina, Khalid Mustafa Ramadan, Muhammad Ijaz Khan, Rajashekhar Choudhari, Rathod Kirankumar Gulab, Iskander Tlili, Kamel Guedri, and Ahmed M. Galal. "Peristaltic activity in blood flow of Casson nanoliquid with irreversibility aspects in vertical non-uniform channel." *Journal of the Indian Chemical Society* 99, no. 8 (2022): 100617. https://doi.org/10.1016/j.jics.2022.100617
[48] Sumalatha, Chenna, and Shankar Bandari. "Effects of radiations and heat source/sink on a Casson fluid flow over nonlinear stretching sheet." *World Journal of Mechanics* 5, no. 12 (2015): 257-265. https://doi.org/10.4236/wjm.2015.512024
[49] Gul, Taza, Ramla Akbar, Zafar Zaheer, and Iraj S. Amiri. "The impact of the Marangoni convection and magnetic field versus blood-based carbon nanotube nanofluids." *Proceedings of the Institution of Mechanical Engineers, Part N: Journal of Nanomaterials, Nanoengineering and Nanosystems* 234, no. 1-2 (2020): 37-46. https://doi.org/10.1177/2397791419872892
[50] Akbar, Noreen Sher, M. Raza, and R. Ellahi. "Influence of induced magnetic field and heat flux with the suspension of carbon nanotubes for the peristaltic flow in a permeable channel." *Journal of magnetism and magnetic materials* 381 (2015): 405-415. https://doi.org/10.1016/j.jmmm.2014.12.087
[51] Kafoussias, N. G., and E. W. Williams. "Thermal-diffusion and diffusion-thermo effects on mixed free-forced convective and mass transfer boundary layer flow with temperature dependent viscosity." *International Journal of Engineering Science* 33, no. 9 (1995): 1369-1384. https://doi.org/10.1016/0020-7225(94)00132-4
[52] Olanrewaju, P. O., and J. A. Gbadeyan. "Effects of Soret, Dufour, chemical reaction, thermal radiation and volumentric heat generation/absorption on mixed convection stagnation point flow on an iso-thermal vertical plate in porous media." *Pacific Journal of Science and Technology* 11, no. 2 (2010): 1-12.
[53] Alam, M. S., M. Ferdows, M. Ota, and M. A. Maleque. "Dufour and Soret effects on steady free convection and mass transfer flow past a semi-infinite vertical porous plate in a porous medium." *Applied Mechanics and Engineering* 11, no. 3 (2006): 535.

[54] Vishalakshi, Angadi Basettappa, Thippaiah Maranna, Ulavathi Shettar Mahabaleshwar, and David Laroze. "An effect of MHD on non-Newtonian fluid flow over a porous stretching/shrinking sheet with heat transfer." *Applied Sciences* 12, no. 10 (2022): 4937. https://doi.org/10.3390/app12104937

[55] Dero, Sumera, T. N. Abdelhameed, Kamel Al-Khaled, Liaquat Ali Lund, Sami Ullah Khan, and Iskander Tlili. "Contribution of suction phenomenon and thermal slip effects for radiated hybrid nanoparticles (Al 2 O 3− Cu/H 2 O) with stability framework." *International Journal of Modern Physics B* 37, no. 15 (2023): 2350147. https://doi.org/10.1142/S0217979223501473

[56] Turkyilmazoglu, Mustafa. "MHD fluid flow and heat transfer due to a stretching rotating disk." *International journal of thermal sciences* 51 (2012): 195-201. https://doi.org/10.1016/j.ijthermalsci.2011.08.016

[57] Yin, Chenguang, Liancun Zheng, Chaoli Zhang, and Xinxin Zhang. "Flow and heat transfer of nanofluids over a rotating disk with uniform stretching rate in the radial direction." *Propulsion and Power Research* 6, no. 1 (2017): 25-30. https://doi.org/10.1016/j.jppr.2017.01.004

[58] Hayat, Tasawar, Farwa Haider, Taseer Muhammad, and Ahmed Alsaedi. "On Darcy-Forchheimer flow of carbon nanotubes due to a rotating disk." *International Journal of Heat and Mass Transfer* 112 (2017): 248-254. https://doi.org/10.1016/j.ijheatmasstransfer.2017.04.123

[59] Akbar, Noreen Sher, and Z. H. Khan. "Heat transfer study of an individual multiwalled carbon nanotube due to metachronal beating of cilia." *International Communications in Heat and Mass Transfer* 59 (2014): 114-119. https://doi.org/10.1016/j.icheatmasstransfer.2014.10.012

[60] Aziz, Arsalan, Ahmed Alsaedi, Taseer Muhammad, and Tasawar Hayat. "Numerical study for heat generation/absorption in flow of nanofluid by a rotating disk." *Results in physics* 8 (2018): 785-792. https://doi.org/10.1016/j.rinp.2018.01.009

[61] Mushtaq, A., and M. Mustafa. "Computations for nanofluid flow near a stretchable rotating disk with axial magnetic field and convective conditions." *Results in physics* 7 (2017): 3137-3144. https://doi.org/10.1016/j.rinp.2017.08.031

[62] Makinde, O. D., and I. L. Animasaun. "Thermophoresis and Brownian motion effects on MHD bioconvection of nanofluid with nonlinear thermal radiation and quartic chemical reaction past an upper horizontal surface of a paraboloid of revolution." *Journal of Molecular liquids* 221 (2016): 733-743. https://doi.org/10.1016/j.molliq.2016.06.047

[63] Makinde, O. D., and I. L. Animasaun. "Bioconvection in MHD nanofluid flow with nonlinear thermal radiation and quartic autocatalysis chemical reaction past an upper surface of a paraboloid of revolution." *International Journal of Thermal Sciences* 109 (2016): 159-171. https://doi.org/10.1016/j.ijthermalsci.2016.06.003